Eur. Phys. J. E **20**, 467–473 (2006)
DOI 10.1140/epje/i2006-10037-9

THE EUROPEAN PHYSICAL JOURNAL E

Temperature dependence of the effective anchoring energy for a nematic-ferroelectric interface

V.A. Gunyakov[a], A.M. Parshin, and V.F. Shabanov

L.V. Kirensky Institute of Physics, Siberian Branch of the Russian Academy of Sciences, Krasnoyarsk 660036, Russia

Received 29 March 2006 and Received in final form 21 July 2006 /
Published online: 5 September 2006 –

Abstract. Specific features of the anisotropic interaction between a nematic mixture and a polar surface of a ferroelectric triglycine sulfate crystal have been studied over a wide temperature range including the substrate's Curie point T_c. The mixture was composed of two nematic liquid crystals, 60% of *p*-methoxybenzylidene-*p*–*n*-butylaniline (MBBA) and 40% of *p*-ethoxybenzylidene-*p*–*n*-butylaniline (EBBA), and doped with a small amount of a dichroic dye. The temperature dependence of the polarized components of optical density D_j of the dye absorption band for the nematic and isotropic phases of the MBBA+EBBA mixture has been obtained using polarization optic techniques. The temperature-induced structural changes in the nematic layer near T_c were found to be related to the changes in the orientational part of the tensor order parameter Q_{ik}. The experimental data have been interpreted using the model, in which the dispersive van der Waals forces of the substrate stabilize the planar orientation of the nematic in the bulk competing with the short-range anchoring forces in the vicinity of T_c. At the same time, the anisotropic part of the surface energy has two terms with the orthogonal easy axes. The nature of the surface electric field and its effect on the director alignment at the interface have been clarified. Taking into account the known relation between anchoring strength and the nematic order parameter, the effective anchoring energy w_{eff} for the studied system has been determined as a function of temperature.

PACS. 61.30.Gd Orientational order of liquid crystals: electric and magnetic field effects on order – 61.30.Hn Surface phenomena: alignment, anchoring, anchoring transitions, surface-induced layering, surface-induced ordering, wetting, prewetting transitions, and wetting transitions – 78.20.Ci Optical constants (including refractive index, complex dielectric constant, absorption, reflection and transmission coefficients, emissivity)

1 Introduction

A typical way to control macroscopic (optical, dielectric, etc.) properties of nematic liquid crystals (LCs) is to use external forces acting on a nematic volume and competing with surface anchoring, which stabilizes a particular orientation of mesogenic molecules [1,2]. An alternative approach to control liquid-crystal orientation involves techniques, which act mostly on a LC-substrate interface [3]. Surface director reorientations caused by competition of counteracting alignment mechanisms are of special interest. These drastic changes of the director orientation are similar to phase transition phenomena and are usually called anchoring transitions [4]. Such transitions are often affected by temperature, which changes the balance of forces on the surface. The transition from planar to homeotropic alignment with varying temperature has been previously observed [5], driven by the competition between dispersive van der Waals and short-range anchoring forces on the surface. The competition between polar and dispersive forces of the substrate also favors the orientational transition [6]. At the same time, the surface electric field of the substrate substantially affects the alignment of LCs because of its dielectric anisotropy and enhances the polar effects at the confining surfaces [7]. The competing effects of dielectric, polar and dispersive forces can be observed on the orienting surfaces of ferroelectrics [8–11]. The spontaneous polarization field of a ferroelectric crystal depends on temperature and vanishes at the transition to the nonpolar state, which occurs at the Curie point T_c. If the mesophase range includes the Curie point T_c, the nematic alignment can be observed until the substrate's electric field completely disappears. It should be noted that using birefringence or ellipsometry techniques to study structural changes in LC cells with crystalline substrates is a challenge, since the optical anisotropy of the substrates modifies the LC response to polarized radiation in an unknown way. Besides, the optical indicatrix of the crystalline substrates may also change

[a] e-mail: gun@iph.krasn.ru

with temperature. This problem can be partially overcome by means of polarization spectroscopy of solute absorption. Introducing a small concentration of a dye with large dichroism to the LC matrix creates an absorption band within the transparent region of the matrix without changing its main properties. This allows to observe the changes of the director orientation and to control the alignment of mesogenic molecules during field-induced or spontaneous structural transformations in nematics [12,13]. Recently, the unusual intensity changes of solute absorption have been observed near T_c in the nematic mixture placed between two ferroelectric substrates [14]. These changes were presumably caused by the surface orientational transition. However, due to the ambiguous temperature behavior of the absorption caused by the proximity ($\sim 2\,^\circ$C) of the nematic to isotropic and ferroelectric to nonpolar state phase transitions, questions about the alignment of nematic molecules above T_c and about the character of the observed transformations remained unanswered. In this paper, we applied the same polarization optic technique to study the surface properties of a nematic mixture with a wider mesophase range. The temperature dependence of the module S of the tensor order parameter Q_{ik} of the mixture was established by using dichroism and refractive-index measurements. We also analyzed the effect of the surface electric field on the director alignment at the boundaries and the behavior of temperature dependence of the effective anchoring energy between the nematic mixture and the ferroelectric substrate.

2 Experimental

A mixture of two nematic LCs, 60% of MBBA (*p*-methoxybenzylidene-*p*–*n*-butylaniline) and 40% of EBBA (*p*-ethoxybenzylidene-*p*–*n*-butylaniline), has been prepared for this study. The mixture had the following phase sequence *Cr*-12 °C-*N*-55.3 °C-*I* showing phase transitions between the crystalline, nematic and isotropic liquid phases. The concentration ratio of the mixture's constituents resulted in substantial increase of the mesophase temperature range. A dichroic dye on the basis of ester of 1, 4-diaminoanthraquinone-2-carboxylic acid (KD-10)

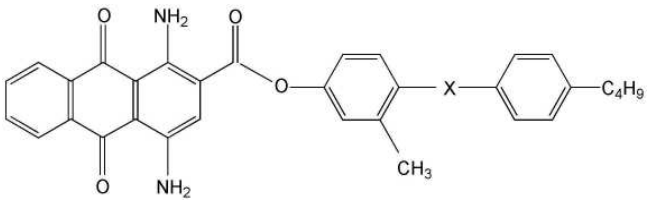

with the absorption band maximum at the wavelength $\lambda = 642$ nm [15] was added to the mixture. The band's nondegenerate long-wave electron $\pi \to \pi^*$ transition, followed by the charge transfer from the amine group to the phenyl ring, is polarized along the longitudinal molecular axis [16]. The small weight concentration ($c_d \sim 0.3\%$) of the dye had no noticeable effect on the clearing point $T_{NI} = 55.3\,^\circ$C, the sample birefringence and the ordering degree of the nematic mixture.

The cells with polar and nonpolar substrates were used in the experiment to orient the nematic mixture. To make the polar substrates, plates of the triglycine sulfate (TGS, $[(NH_2CH_2COOH)_3H_2SO_4]$) crystal with typical domain structure corresponding to the minimum of the ferroelectric's free energy [8], were split along the cleavage plane normal to the ferroelectric axis $\boldsymbol{b}$. Planar mixture layers under study were doped by dichroic dye KD-10 and placed between two coaxial $8 \times 5 \times 0.5$ mm TGS plates containing the "−" domains. Since the size of the domains was about 1–3 mm, it is very unlikely that they could influence the response of the LC (for a detailed description of the domain structure, see [8]). The director $\boldsymbol{n}$ of the mixture was parallel to the crystallographic $\boldsymbol{c}$-axes of TGS. The cell parameters and the sample preparation technique were the same as in [14]. The cell region exposed to probing radiation was chosen using a diaphragm with a diameter of 2 mm. The polarized components of optical density D_j of the dye-doped mixture for the TGS cells were obtained with an automated spectrometer KSVU-23 at fixed temperature $T = 23\,^\circ$C. The temperature behavior of the components D_j was then studied on the polarization optic system [13] based on a He–Ne laser ($\lambda = 633$ nm). Since the dichroic ratio $N(\lambda) = D_\parallel(\lambda)/D_\perp(\lambda)$ for the above-mentioned band is independent of λ [16], the one-beam scheme was used. Further in text, the indices $\parallel, \perp, i$ correspond to the direction parallel ($\parallel$) or perpendicular ($\perp$) to the nematic director $\boldsymbol{n}$, and to the isotropic liquid (i), respectively. To record the components $D_{||,\perp}$, the director of the sample was oriented, respectively, parallel or perpendicular to the polarization direction of light passing through the sample. The accuracy of adjusting the direction of $\boldsymbol{n}$ relative to the polarization vector of light wave $\boldsymbol{e}$ was about $\pm 1°$. The contribution of the background radiation caused by light scattering from the anisotropic substrates was excluded by subtracting the corresponding contribution of the radiation passing through the sample part free of the nematic mixture. This procedure was done independently for each component of optical density in every temperature point. The temperature uniformity over the whole sample volume and the thermal stability within the mesophase range was not worse than $\pm 0.1\,^\circ$C.

When the director field along the z-axis (normal to the substrate) is distorted, some effective optical density D_e is recorded instead of $D_{||}$ [12]. Figure 1 shows the experimental dependences of D_e and $D_\perp$ on the reduced temperature $\Delta T = T_{NI} - T$ for the TGS cell, averaged over a series of samples. Provided for the comparison are the temperature dependences $D_{\parallel,\perp}(\Delta T)$ of the dye-doped mixture for the cell of the same thickness with nonpolar glass substrates. One can see that within the major portion of the mesophase range the optical density D_e of the TGS cell coincides with $D_\parallel$. However, the two curves diverge sharply in the vicinity of T_c. A significant difference between the values of D_e and $D_\parallel$, exceeding the accuracy of their experimental measurements, was observed at temperature $T^+ \approx 42\,^\circ$C. Above T_c, the optical density

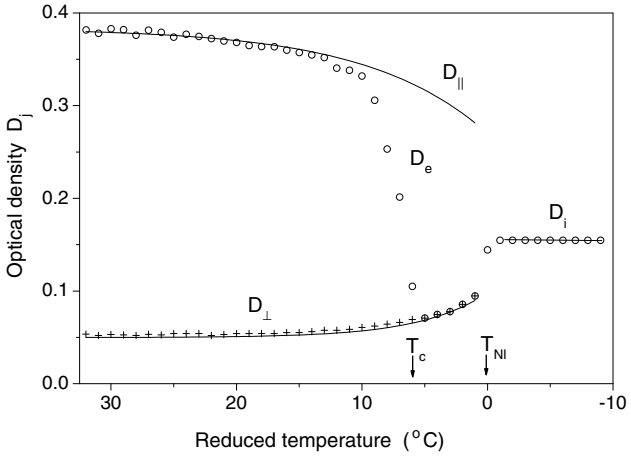

Fig. 1. The temperature curves of the polarized components D_j of the KD-10 dye absorption band for the nematic and isotropic phases of the MBBA+EBBA mixture: D_e (○) and $D_\perp$ (+) in the TGS cell, $D_{\parallel,\perp,i}$ (solid lines) in the glass cell; the cell thickness $d = 20\,\mu$m, the dye concentration $c_d = 0.3$ wt%. Arrows indicate the Curie point T_c and the clearing point T_{NI}.

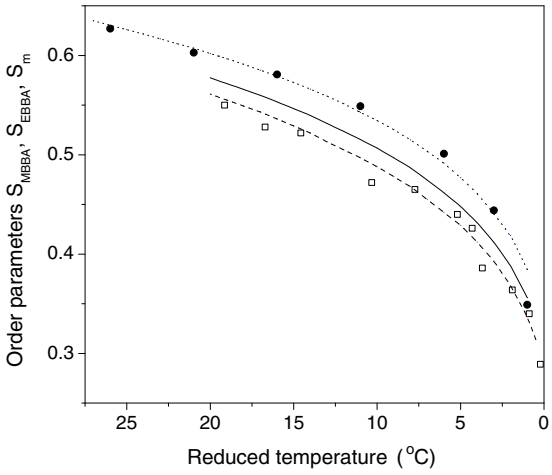

Fig. 2. The temperature dependences of the orientational order parameters $S_{\rm MBBA}$, $S_{\rm EBBA}$, and S_m in the nematic phase: MBBA (□), the NMR data from [17] and its Haller approximation [19] (dashed line); EBBA (•), the NMR data from [18] and its Haller approximation (dotted line); the MBBA+EBBA mixture data (solid line) calculated from equation (1).

D_e coincides with $D_\perp$, and finally, above T_{NI}, it coincides with the density of the isotropic phase D_i.

The analysis of the experimental spectra requires information about the orientational order parameter and the dispersion of the refractive indices of the orienting nematic matrix. The values of the order parameters $S_{\rm MBBA}$ (squares) and $S_{\rm EBBA}$ (solid circles) as functions of temperature, obtained from the published NMR data [17,18], are given in Figure 2. The dashed line is Haller's approximation of $S_{\rm MBBA}(T)$ calculated using $S = S_0(1 - T/T^*)^\beta$ with the fitting parameters $S_0 = S(T = 0)$, $(T^* - T_{NI}) = 0.92$, and $\beta = 0.213$ [19]. The same procedure with the values $(T^* - T_{NI}) = 0.6$ and $\beta = 0.181$ was used to approximate the dependence of $S_{\rm EBBA}(T)$ (dotted line). The

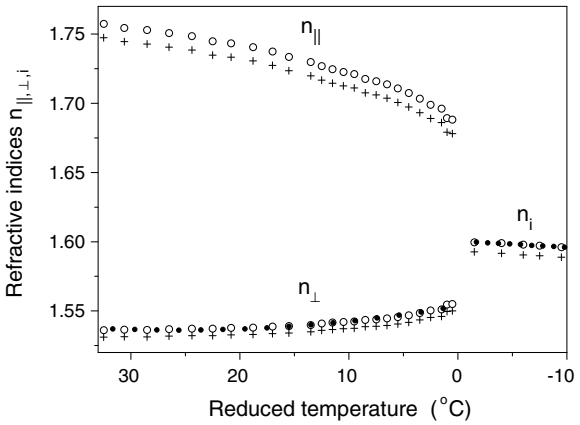

Fig. 3. The refractive indices $n_{\parallel,\perp,i}$ of the MBBA+EBBA mixture as a function of reduced temperature at the wavelengths $\lambda = 589$ nm (○) and 633 nm (+). The solid circles (•) show the values of $n_{\perp,i}$ measured with the refractometer (589 nm).

mixture order parameter S_m (solid line) was calculated from equation [19]

$$S_m(T) = cS_{\rm MBBA}(T) + (1 - c)S_{\rm EBBA}(T), \qquad (1)$$

where c is the molar fraction of MBBA. The refractive indices $n_{\parallel,\perp,i}$ of the MBBA+EBBA mixture at wavelengths 589 nm and 633 nm were obtained by the prism technique using a goniometer [20]. Their temperature dependences are shown in Figure 3. The refractive indices $n_{\perp,i}$ were also measured with an Abbe refractometer (IRF-454B). A good agreement between the experimental data obtained with the goniometer and the refractometer indicated that the prism technique was applied correctly. A precision for the measured refractive indices was found to be about 10^{-3}.

3 Results and discussion

It was assumed earlier [14] that the most probable explanation of the unusual absorption behavior of the TGS cell is a reorientation of LC molecules from the planar to homeotropic texture, *i.e.* an orientational transition. Indeed, the change of optical anisotropy of the ferroelectric substrates with temperature is negligibly small over the whole mesophase range of the studied mixture [21] and, therefore, could not lead to the considerable optical density changes seen in Figure 1. On the other hand, it is known that the orientational statistics of a uniaxial nematic phase is described in terms of the tensor order parameter [1]

$$Q_{ik} = S\left(n_i n_k - \frac{1}{3}\delta_{ik}\right), \qquad i,k = x,y,z. \qquad (2)$$

Here, the module $S = (3\overline{\cos^2\theta} - 1)/2$ is a scalar uniaxial order parameter, the horizontal bar represents statistical averaging over all molecules, $n_{i,k}$ are the components of the macroscopic director $\boldsymbol{n}$, and $\delta_{ik} = 1$ if $i = k$ and 0

if $i \neq k$. Any change in Q_{ik} resulting from an external perturbation can be reduced to the changes of the module S, the direction of $\boldsymbol{n}$ or both. Hence, it is important to know whether the only change is in the direction of $\boldsymbol{n}$ or the module S changes as well. For this purpose, the temperature dependence of the solute order parameter S was found using the results of two independent experiments. In the ferroelectric region of the substrate below T^+ the parameter S was obtained from the relation [19]

$$S = \frac{N_1 g_1 - 1}{N_1 g_1 + 2}, \tag{3}$$

where the dichroic ratio $N_1 = D_{||}/D_\perp \equiv D_e/D_\perp$. In the temperature range $T^+ < T < T_{NI}$, including T_c and the nonpolar phase of the substrate, the parameter S was determined from the relation [19]

$$S = 1 - N_2 g_2, \tag{4}$$

where the dichroic ratio $N_2 = D_\perp/D_i$. The correction factors $g_{1,2}$ take into account the anisotropy of the local field of the light wave [19],

$$g_1 = \frac{n_{||}}{n_\perp}\left(\frac{f_\perp}{f_{||}}\right)^2, \qquad g_2 = \frac{\rho_i n_\perp}{\rho n_i}\left(\frac{f_i}{f_\perp}\right)^2. \tag{5}$$

Here $n_{||,\perp,i}$ are the background refractive indices within the dye absorption band coinciding with those of the matrix and $f_{||,\perp,i}$ are the background components of the local-field tensor for solute molecules within their absorption band. The anisotropy of the local-field tensor for MBBA was found to be negligibly small [22]. Thus, the approximation of an isotropic local field ($f_\perp/f_{||} \approx 1$, $f_i/f_\perp \approx 1$) was accepted for the mixture of MBBA with its ethoxy homologue. The values of the refractive indices at wavelength $\lambda = 633\,\mathrm{nm}$ used to calculate the factors $g_{1,2}$ were taken from Figure 3. The densities ρ and ρ_i for the nematic and isotropic phases of MBBA were taken from [20].

The temperature dependence of the order parameter S of the KD-10 dye molecules in the nematic phase of the MBBA+EBBA mixture is shown in Figure 4. The order parameter S was calculated according to equation (3) in the temperature range $T < T^+$ and according to equation (4) in the temperature range $T^+ < T < T_{NI}$. As seen in Figure 4, the dependence $S(T)$ is monotonic and not sensitive to the transition of the ferroelectric substrate to the nonpolar state within the experimental error. Thus, the specific behavior of D_e, seen in Figure 1, is caused by the changes of the orientational part of the tensor order parameter Q_{ik} implying the purely orientational transition. The continuous form of the dependence $S(T)$ at the conjunction point T^+ also suggests that the isotropic local-field approximation is valid for the studied mixture.

To find out if the director pattern is homogeneous under conditions of the orientational transition, we used the magnetic null method [23] to determine the tilt angle across the sample at certain temperature points within the $T^+ < T < T_c$ range. However, we could not detect the position, where the optical transmission of the TGS cell did not change upon applying the external magnetic field. This result led us to conclude that the deformation across the nematic layer corresponds to the nonuniform distribution of the director.

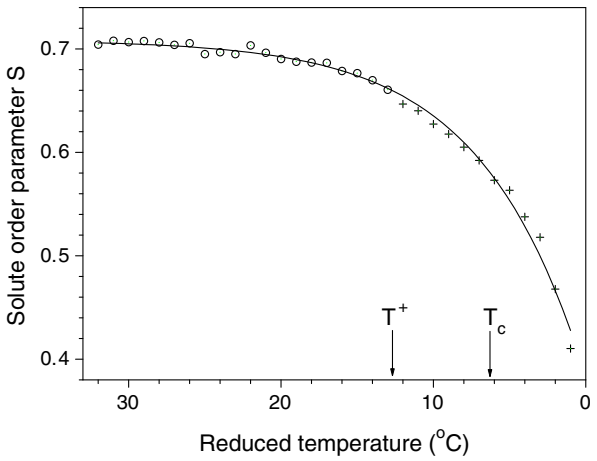

Fig. 4. The orientational order parameter S of the KD-10 dye molecules in the nematic phase of the MBBA+EBBA mixture as a function of reduced temperature: open circles (○) show the values of S calculated from equation (3), crosses (+) show those calculated from equation (4); the solid line is the interpolation. The temperature curves $S(T)$ merge at the conjunction point $T^+ \approx 42\,^\circ\mathrm{C}$.

Let us analyze contributions of the surface energy, which could take place in the system under study. First, we limit our analysis by the vicinity of the point T^+, where nematic director deformations are small and the Rapini-Papoular approximation is valid [7]. It is well known that the substrate's electric field is induced by surface charges, which are due to the spontaneous polarization P_S of the ferroelectric crystal. A nematic energy density in the presence of surface electric field $\boldsymbol{E} = E(z)\boldsymbol{l}$, where $\boldsymbol{l}$ is the unit vector parallel to the z-axis, can be described as [24]

$$-\frac{1}{2}\varepsilon_a \varepsilon_0 (\boldsymbol{E}\cdot\boldsymbol{n})^2 - q\frac{\partial E_z}{\partial z} n_z^2. \tag{6}$$

Here $\varepsilon_a = \varepsilon_{||} - \varepsilon_\perp$ is the dielectric anisotropy of the nematic, ε_0 is the permittivity of vacuum, q is the difference between the longitudinal and transverse components of the quadrupole electric moment density tensor in the nematic and $\boldsymbol{n}$ is the director. The first term in equation (6) comes from the dielectric energy contribution while the second, quadrupolar term, takes into account the nonuniformity of the surface electric field. Two terms of electric origin appearing in equation (6) are usually of the same order of magnitude [7]. However it has been previously established [9] that the nonuniformity of the substrate electric field has no significant influence on the nature of the interaction between MBBA and the TGS cleavage surface. To explain this phenomenon, the authors of reference [9] suggest that the field of polarization charges on the TGS cleavage is screened by the ions present in any nematic material. Therefore, we can assume, as a first approximation, that the corresponding energy per unit area is connected

with the first term appearing in equation (6),

$$f_e = -\frac{1}{2}\varepsilon_a\varepsilon_0 \int_0^\infty E^2(z)\cos^2\theta(z)\mathrm{d}z, \tag{7}$$

where $\theta = \cos^{-1}(\boldsymbol{n}\cdot\boldsymbol{l})$. The presence of ions should induce a double electric layer, similar to that of a weak electrolyte, near the interface, beyond which the surface field quickly vanishes. For a nematic LC, the density of ions adsorbed on the confining surfaces usually does not exceed 0.8–1.5 $\times 10^{-7}$ C/cm^2 [7,25]. At the same time, the density of polarization charges on a fresh TGS cleavage can be as high as 2.8×10^{-6} C/cm^2 at room temperature [26]. Evidently, the nematic ions deposited on the cleavage can only partially screen the field of polarization charges. On the other hand, compensation of polarization charges on the TGS surface rapidly occurs due to charge carriers trapped at the surface states and to transfer of carriers from the bulk of the ferroelectric substrate [27]. These processes result in complete screening of the bound charges on the domain surface [28]. Thus, for samples in the state of thermodynamic equilibrium, the electric field acting on the nematic molecules is presumably due to the density of adsorbed ions σ_{LC} of LC and can be written as

$$E(z) = \frac{\sigma_{\mathrm{LC}}}{\varepsilon\varepsilon_0}\exp(-z/\lambda_D), \tag{8}$$

where $\varepsilon = (\varepsilon_{||} + 2\varepsilon_\perp)/3$ is the mean dielectric constant of the LC and z is the distance from the substrate. The electric field is normal to the surface and penetrates into the LC to the depth of the Debye length λ_D. In terms of the Debye-Huckel theory, this parameter has the following form [29]:

$$\lambda_D = \sqrt{\frac{\varepsilon\varepsilon_0 k_B T}{2q_e\rho_0}}, \tag{9}$$

where q_e is the proton charge, k_BT is the thermal energy and ρ_0 is the volume density of LC charges. For nematic materials, ρ_0 has a typical value $\rho_0 = 0.6 \times 10^{-5}$ C/cm^3 [25]. The values of the dielectric constant for the mixture were calculated from the published data for MBBA and EBBA [30] using the relation $\varepsilon(T) = c\varepsilon_{\mathrm{MBBA}}(T) + (1-c)\varepsilon_{\mathrm{EBBA}}(T)$ [2], where c is the molar fraction of MBBA. The temperature dependences of $\varepsilon_{||,\perp}$ for the mixture and its components are shown in Figure 5. These data allow us to calculate the mean value and the anisotropy of the mixture's dielectric constant over the whole mesophase range. Taking $\varepsilon = 4.87$ at $T = 23\,^\circ$C, we find from equation (9) that the surface electric field penetrates into the LC to the depth $\lambda_D \sim 0.3\,\mu$m. Although the surface electric field $\boldsymbol{E}$ is a nonlocal quantity, according to Barbero and Durand [7] the corresponding orientational dielectric free energy can be considered as quasi-local and simply renormalizes the interfacial properties of the nematic-ferroelectric system. According to equation (7), if $\mathrm{d}\theta/\mathrm{d}z = 0$, the dielectric relation between the surface field and the nematic director contributes the term $-(1/2)\cdot w_{el}\cos^2\theta$ to the surface free energy, with the

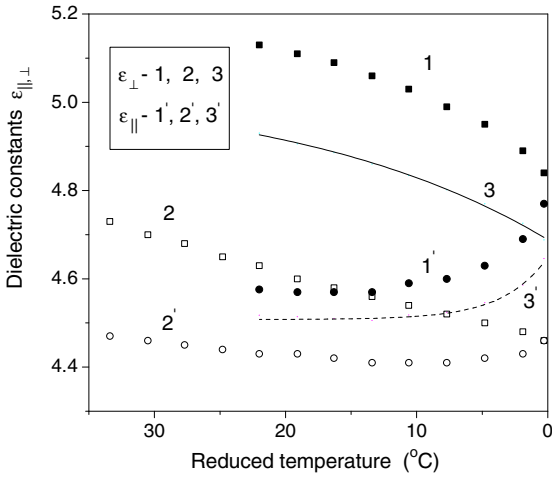

Fig. 5. The temperature dependences of the dielectric constants $\varepsilon_{||,\perp}$ for MBBA $(1,1')$, EBBA $(2,2')$ and the MBBA+EBBA mixture $(3,3')$.

coefficient [7]

$$w_{el} = \frac{\varepsilon_a}{2\varepsilon_0}\frac{\sigma_{\mathrm{LC}}^2}{\varepsilon^2}\lambda_D. \tag{10}$$

For $\varepsilon_a < 0$, which is the case for the MBBA+EBBA mixture, the dielectric energy w_{el} stabilizes nematic planar anchoring on the TGS cleavage surface. As temperature increases, the dielectric contribution decreases, vanishing at T_c. The van der Waals dispersion forces of the substrate favor the planar texture, since they are responsible for the different nematic alignment on the "+" and "–" domains of TGS [24]. Thus, the contributions from the electric field and the dispersion forces give rise to torques within the surface plane. At the same time, the asymmetric effect of the solid crystal - LC interface and the nature of the interaction between the ends of molecules and the TGS cleavage surface [31] may give rise to a torque, which favors the homeotropic alignment. Under the vanishing field condition, this factor makes an important contribution to the surface free energy of the nematic, competing with the dispersive van der Waals forces at the boundaries. According to [32], this contribution takes the following form: $f_0 = -(1/2)w_0\cos^2\theta$, where the coefficient w_0 serves as the anchoring energy. Taking this into consideration, the total energy per unit surface, which plays the role of the effective anchoring energy for the studied system, can be presented as

$$w_{eff} = w_0 + \frac{\varepsilon_a}{2\varepsilon_0}\frac{\sigma_{\mathrm{LC}}^2}{\varepsilon^2}\lambda_D. \tag{11}$$

Evidently, the temperature behavior of w_{eff} will depend on the two terms resulting in the orthogonal easy axes on the ferroelectric surface. It is well known that the temperature dependence of the first term is determined by the squared nematic order parameter, *i.e.* $w_0(T) \approx a\cdot S_m^2(T)$ [33,34] with some constant a. The temperature dependence of the second term exhibits a more complicated nature. The values ε_a, ε and σ_{LC} are functions of

Table 1. Experimental data for the computation of the parameters a and b.

ΔT (°C)	w_{eff} (J/m^2)	ε_a	ε	P_S (C/cm^2)	S_m
13	0 [35]	−0.35	4.74	$1.71 \cdot 10^{-6}$ [26]	0.531
32	$2.1 \cdot 10^{-5}$ [10]	−0.44	4.87	$2.76 \cdot 10^{-6}$ [26]	0.632

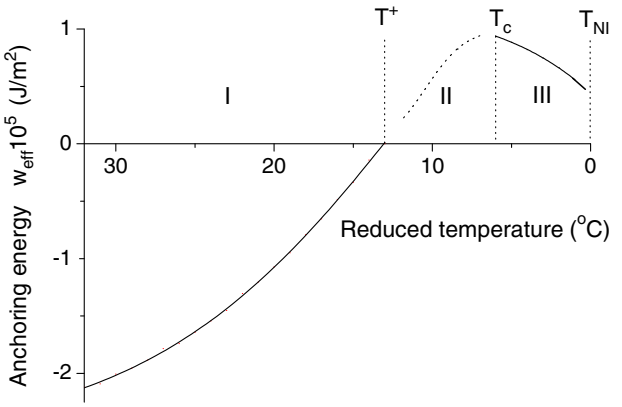

Fig. 6. The nonmonotonic temperature dependence of the effective anchoring energy w_{eff} for the MBBA+EBBA mixture over the mesophase range including the ferroelectric and nonpolar phases of the TGS substrate: I) $w_{eff} < 0$, planar alignment (solid line); II) $w_{eff} > 0$, unknown nonuniform alignment (dashed line); III) $w_{eff} \equiv w_0$, homeotropic alignment (solid line).

temperature. Since an ion adsorption in LC during its contact with a ferroelectric substrate is induced by the spontaneous polarization of the ferroelectric, their temperature behavior must be closely related. As a first approximation, we assumed a relation $\sigma_{\mathrm{LC}}(T) \approx b \cdot P_S(T)$ with some constant coefficient b. An estimation of λ_D from equation (9) shows that the magnitude of this parameter remains essentially constant over the temperature range below T_c. On the other hand, the values of w_{eff} for the studied system can be evaluated at least in two temperature points. Previously we determined experimentally [10] that w_{eff} has a value $w_{eff} = (2.1 \pm 0.1) \times 10^{-5}$ J/m^2 at room temperature ($\Delta T = 32\,^\circ$C). The second point ($\Delta T = 13\,^\circ$C) has been ascertained, assuming that the competing terms cancel each other ($w_{eff} = 0$) at the temperature-induced anchoring transition [35]. The data required to compute the fitting parameters a and b are presented in Table 1. Using these data and solving the combined equations, we found $a = 4.4 \times 10^{-5}$ J/m^2 and $b = 16 \times 10^{-5}$. Then, using the order parameter and dielectric constant data from Figures 2 and 5, respectively, and the published temperature dependence of P_S [26], equation (11) allowed us to calculate the values of w_{eff} from room temperature up to the point T_{NI}. The temperature dependence of the anchoring energy w_{eff} can be described in terms of the three regions I–III, bordered by the critical points T^+, T_c, and T_{NI}, and is presented in Figure 6.

In region I, the values $\mathrm{d}\theta/\mathrm{d}z = 0$ and $w_{eff} < 0$ correspond to the planar alignment of the nematic director. At the critical point T^+, separating regions I and II, $w_{eff} = 0$ and the uniform orientation $\mathrm{d}\theta/\mathrm{d}z = 0$ must be preserved. In region II, as we showed experimentally with the magnetic null method, the derivative $\mathrm{d}\theta/\mathrm{d}z \neq 0$. We believe that, in this region, a nonuniform deformation of the nematic layer in the TGS cell is caused by the competition between the dispersive and polar forces near the surface and by the reduction of the substrate's electric field until its complete disappearance at the Curie point T_c. The long-range dispersive van der Waals forces are known to create volume torques, which stabilize the orientation of the nematic molecules according to the surface symmetry of the crystalline substrates [36]. As shown in [36], the potential U describing the van der Waals torques, is roughly proportional to the nematic order parameter S_m. The comparison of the temperature dependences of the derivatives of S_m and S_m^2 with respect to T, obtained using the data from Figure 2, clearly indicates that in the interval $T^+ < T < T_c$ the van der Waals potential $U \sim S_m$ drops quite faster than the short-range anchoring forces $w_0 \sim S_m^2$. Presumably, due to reduction of the potential U, the dispersive forces can no longer stabilize the planar orientation of the LC molecules in the cell volume, and the short-range anchoring forces begin to dominate inducing a uniform orientation of the nematic molecules across the sample above T_c.

In the interval $T^+ < T < T_c$, we have a case, where the director is not close to the easy axis, so the torque balance equation for the nematic layer at the surface including non-Rapini anchoring contributions can be written as

$$K\frac{\mathrm{d}\theta}{\mathrm{d}z} = -\frac{w_2}{2}\sin 2\theta_0 - \sin\theta_0 \sum_{n=2}^{\infty} n w_{2n} \cos^{2n-1}\theta_0, \quad (12)$$

where $K = K_{11} = K_{22} = K_{33}$ is the average Frank elastic constant, and θ_0 is the nematic director orientation at the surface; w_2 is the effective anchoring energy w_{eff} represented by equation (11) and w_{2n} are the non-Rapini anchoring contributions [37–39]. Presumably, the presence of the non-Rapini terms in the surface potential results in the continuous transition from planar to tilted to homeotropic alignment, which was observed for the studied system earlier [35]. However, the dependence $w_{eff}(T)$ for this region could not be determined exactly because of the unknown function $\theta(z)$ and the values of w_{2n}. Therefore, we have qualitatively presented it as a dashed curve in Figure 6.

Finally, in region III, $\mathrm{d}\theta/\mathrm{d}z = 0$ and $w_{eff} \equiv w_0 > 0$ and $\theta_0 = 0$ in agreement with equation (12), corresponding to the homeotropic alignment of the nematic director. Thus, the reorientation of the nematic director inside the TGS cell from the planar to homeotropic texture through the intermediate interval with a deformed nematic layer is occurred. A model used in this study can be applied to describe the specific features of the anisotropic interaction

between a nematic and a polar surface of a ferroelectric crystal. It should be noted that actual values of the angle θ_0 for the studied system can be presumably obtained by establishing the relation between $\mathrm{d}\theta/\mathrm{d}z$ and the magnitude of the optical density D_e. This work is in progress and will be presented elsewhere.

4 Conclusion

In this study, we have clarified the mechanism of the critical behavior of the nematic MBBA+EBBA mixture on the ferroelectric TGS substrate in the vicinity of the substrate's Curie point T_c. The nematic orientation results from the competition of the two alignment mechanisms. The substrate's electric field attempts to "lay" the nematic molecules onto the substrate plane, while the polar effects favor the homeotropic texture. In the temperature range corresponding to the polar state of TGS the interaction between the nematic molecules and the substrate is mainly due to the dielectric term of the surface free energy. This term, in turn, is governed by the value of the density of LC ions adsorbed onto the ferroelectric crystal surface. As a result of the different temperature dependences of the competing factors, the anchoring transition occurs at some temperature T^+. As the sample is heated even further, this transition leads to the structural changes over the entire nematic volume of the TGS cell. It has been shown experimentally that the deformation across the nematic layer corresponds to the nonuniform distribution of the director. In the temperature range corresponding to the nonpolar state of TGS an interaction between the nematic and the substrate is described in terms of anchoring energy and is changed with temperature proportionally to the squared order parameter S_m^2 of the nematic mixture. Thus, both the experimental data and the torque balance analysis indicate a nontrivial temperature dependence of the effective anchoring energy for the studied system. This dependence is interpreted using the model, in which the long-range dispersive van der Waals forces of the crystalline substrate stabilize the planar alignment of the nematic in the bulk competing with the short-range anchoring forces in the vicinity of T_c. At the same time, the anisotropic part of the surface energy has two terms with the orthogonal easy axes. In conclusion we note, that it would be interesting to find out if a nematic-ferroelectric interface can facilitate an anchoring transition, whose critical behavior is different from that of the studied system.

This work was supported by the grants No. 05-03-32852 of RFBR, No. 8.1 of Presidium of the RAS and No. 2.10.2 of DPS of the RAS, No. 02.445.11.7262 of Federal Special Science and Technical Programme, SS-6612.2006.3.

References

1. P.G. de Gennes, J. Prost, *The Physics of Liquid Crystals* (Clarendon Press, Oxford, 1993).
2. L.M. Blinov, V.G. Chigrinov, *Electrooptic Effects in Liquid Crystal Materials* (Springer-Verlag, New York, 1994).
3. L. Komitov, J. Soc. Inf. Display **11**, 437 (2003).
4. B. Jerome, Rep. Prog. Phys. **54**, 391 (1991).
5. G. Ryschenkow, M. Kleman, J. Chem. Phys. **64**, 404 (1976).
6. J.D. Parsons, Phys. Rev. Lett. **41**, 877 (1978).
7. G. Barbero, G. Durand, in *Liquid Crystals in Complex Geometries,* edited by G.Ph. Crawford, S. Zumer (Taylor & Francis, London, 1996); J. Phys. (Paris) **51**, 281 (1990).
8. L.I. Dontzova, N.A. Tikhomirova, L.A. Shuvalov, Ferroelectrics **97**, 87 (1989).
9. M. Glogarova, G. Durand, J. Phys. (Paris) **49**, 1575 (1988).
10. V.A. Gunyakov, A.M. Parshin, V.F. Shabanov, Solid State Commun. **105**, 761 (1998).
11. J.F. Hubbard *et al.*, J. Mater. Chem. **9**, 375 (1999).
12. E.M. Aver'yanov, V.G. Rumyantsev, V.M. Muratov, Opt. Spectrosc. **69**, 128 (1990).
13. V.A. Gunyakov *et al.*, J. Opt. Technol. **64**, 483 (1997).
14. A.M. Parshin, V.A. Gunyakov, V.F. Shabanov, JETP Lett. **76**, 299 (2002).
15. A.V. Ivashchenko, V.G. Rumyantsev, Mol. Cryst. Liq. Cryst. A **150**, 1 (1987).
16. H. Inoue *et al.*, Bull. Chem. Soc. Jpn. **45**, 1018 (1972).
17. A. Pines, J.J. Chang, Phys. Rev. A **10**, 946 (1974).
18. J.S. Prasad, J. Chem. Phys. **65**, 941 (1976).
19. E.M. Aver'yanov, *Local Field Effects in Optics of Liquid Crystals* (Nauka, Novosibirsk, 1999).
20. M.F. Vuks, *Electrical and Optical Properties of Molecules and Condensed Matters* (Leningrad University Publishing House, Leningrad, 1984).
21. J. Etxebarria, J. Ortega, T. Breczweski, J. Phys.: Condens. Matter. **4**, 6851 (1992).
22. E.M. Aver'yanov, A.N. Primak, Opt. Spectrosc. **61**, 1040 (1986).
23. H.A. van Sprang, R.G. Aartsen, J. Appl. Phys. **56**, 251 (1984).
24. N.A. Tikhomirova *et al.*, Sov. Phys. Crystallogr. **23**, 701 (1978).
25. R.N. Thurston *et al.*, J. Appl. Phys. **56**, 263 (1984).
26. S. Hoshino *et al.*, Phys. Rev. **107** 1255 (1957).
27. N.A. Tikhomirova *et al.*, Phys. Solid State **28**, 3319 (1986).
28. M.E. Lines, A.M. Glass, *Principles and Application of Ferroelectrics and Related Materials* (Clarendon Press, Oxford, 1977).
29. U. Kuhnau *et al.*, Phys. Rev. E **59**, 578 (1999).
30. Z.Yu. Gotra *et al.*, *Indicated Devices on Liquid Crystals* (Sov. Radio, Moscow, 1980).
31. A.G. Petrov, A. Derzhanski, Mol. Cryst. Liq. Cryst. Lett. **41**, 41 (1977).
32. M.A. Osipov, T.J. Sluckin, S.J. Cox, Phys. Rev. E **55**, 464 (1997).
33. C. Rosenblatt, J. Phys. **45**, 1087 (1984).
34. L.M. Blinov, A.Yu. Kabaenkov, Sov. Phys. JETP **66**, 1002 (1987).
35. V.A. Gunyakov, A.M. Parshin, V.F. Shabanov, Liq. Cryst. **33**, 645 (2006).
36. E. Dubois-Violette, P.G. de Gennes, J. Phys. Lett. **36**, L-255 (1975).
37. K.H. Yang, C. Rosenblatt, Appl. Phys. Lett. **43**, 62 (1983).
38. H. Yokoyama, H.A. van Sprang, J. Appl. Phys. **57**, 4520 (1985).
39. M. Nobili, G. Durand, Phys. Rev. A **46**, R6174 (1992).